Electron polarization and formation probability of bound muonium in CdS and Si

H. V. Alberto,* R. C. Vilão, J. Piroto Duarte,† and J. M. Gil
CEMDRX, Department of Physics, University of Coimbra, P-3004-516 Coimbra, Portugal

A. Weidinger
Helmholtz-Zentrum Berlin für Materialien und Energie, 14109 Berlin, Germany

J. S. Lord and S. F. J. Cox
ISIS Facility, Rutherford Appleton Laboratory, Chilton, Oxon OX11 0QX, United Kingdom
(Received 15 May 2012; revised manuscript received 21 June 2012; published 6 July 2012)

Positive muons implanted in CdS and Si create electrically active defect centers that mimic and model the contrasting donor states of interstitial hydrogen in these two materials—a shallow donor in CdS and a deep donor in Si. In the present experiment the polarization of the muonium electron and the formation probability of these states are investigated. We find that the polarization is rather weak and strongly deviates from the polarization expected for a paramagnetic center at low temperatures and high magnetic fields. We assume that the polarization is built up in a precursor stage and is not completed at the time of conversion to the observed final state. The polarization depends on the purity of the samples and is larger for samples with a higher concentration of defects. In addition, the branching ratio between paramagnetic muonium and diamagnetic muon depends on the purity of the samples and on the strength of the magnetic field. These different findings are interpreted in the following model: after implantation, the muon comes to rest at an interstitial site in the unrelaxed lattice. This site is unstable and relaxes to the final configuration. The total energy along the transition path and the strength of the single electron binding to the positive muon during the transformation determine the parameters of the experiment.

DOI: 10.1103/PhysRevB.86.035203 PACS number(s): 76.75.+i, 72.80.Cw, 72.80.Ey, 75.20.Ck

I. INTRODUCTION

Muonium—the exotic atom composed by an electron bound to a positive muon—is an important source of information of isolated hydrogen behavior in semiconductors.[1,2] Although the muon is only one-ninth the mass of the proton, the reduced mass of muonium is 99.6% of that of hydrogen, so that the respective electronic properties are the same in both atoms.[1,3] In the course of muon implantation experiments, muonium may end up in different charge states and/or configurations relevant to the understanding of the physics of hydrogen in semiconductors. The muon spin rotation (μSR) technique is able to identify the final electronic structure via hyperfine spectroscopy of the neutral (paramagnetic) states. The formation probabilities of the different charged states may also be measured. For example, both the donor and the acceptor configurations have been identified in a variety of semiconductors: both in the elemental[1] in compound III-V (Ref. 4) and compound II-VI (Refs. 5–9) or more recently in several oxides.[10–14]

Muonium formation involves electron capture and equilibration in the lattice structure. Two processes are known:[1] (i) prompt (epithermal) muonium formation where the yield of muonium is defined at the end of the thermalization process, and (ii) delayed muonium formation where muonium may form at a later stage due to interaction with electrons from the radiolysis track. Examples of delayed muonium formation include shallow muonium in II-VI compounds[15,16] and bond-centered (BC) muonium in Si and GaN[1,17–20] but the details of the delayed muonium formation route are, however, still not well known. The understanding of these processes is important both from the point of view of the physics of the late stages of the muon implantation and for the interpretation of the final configurations and their analogy with isolated monatomic hydrogen centers.

Recent measurements of the electron polarization of the muonium state have emerged as a tool to extract information about the processes immediately following muon implantation.[16,21] Electron polarization in CdTe and CdS was measured through the relative intensity of the two shallow muonium lines corresponding to spin-up and spin-down electrons, respectively.

A surprising result of the experiment was that electron polarization does not follow the Boltzmann distribution of spin states expected for a paramagnetic center at low temperatures and high magnetic fields. We found instead that the polarization is weaker than expected and can even change sign upon sample annealing. The explanation of this behavior is that the polarization is built up in the time interval (several 100 ps) between the implantation of the muon and the formation of the final bound state and the buildup process is not completed at the time of the conversion. In addition, two different formation routes were identified, one via a direct conversion from deep to shallow muonium and one via electron capture from the conduction band.

In the present work, we present new polarization data both in CdS and in Si. In CdS, new data are considered for a sample with a high concentration of defects, for which very scarce information was previously available,[16] and the formation probabilities of the different states are evaluated and discussed.

The subject of the electron polarization of BC muonium in Si is addressed here for the first time and shows that the phenomenon of spin polarization of the muonium electron is not restricted to the shallow donor states observed in the II-VI compounds. The electronic structure of muonium

 ©2012 American Physical Society

is extended in CdS (obeying effective mass theory) but is compact (corresponding to a level lying deeper in the gap) in Si. This suggests that the information carried by the spin polarization regarding the precursor states may be accessed in a far larger variety of compounds. Being one of the most relevant semiconductors, Si has been studied extensively by μSR in the past,[1,2] but no polarization data exist so far. A float zone and a Czochralski grown Si sample, both nominally undoped, have been investigated. The experiments show a different polarization for the two samples.

We focus on the BC muonium in Si in these experiments since it can be measured in the Paschen-Back region at high fields where the hyperfine lines correspond to muon spin transitions with well-defined electron spin-up or spin-down states, thus simplifying the analysis. For normal (interstitial) muonium in Si, which is also formed to some extent in these experiments, the polarization measurement and the analysis would be more difficult. The formation probabilities of the BC muonium and of the diamagnetic state were measured and found to be sample dependent.

The electron polarization and the formation probabilities of the different states (paramagnetic or diamagnetic muonium) give important information about the end stage of the muon implantation. In these materials the muon is likely to form a transient (precursor) state for a short time before it finds its final position in the relaxed lattice. The properties of this precursor state and its lifetime determine the parameters measured in the experiment.

Delayed muonium formation and the dependence of the formation probability on the external electric and magnetic field have been studied extensively by Storchak and collaborators.[18] In their model a "weakly bound state," formed after electron capture by the positive muon, plays a decisive role. We interpret our data also in the context of a weakly bound state but we suggest a different origin for this state.

II. EXPERIMENTAL DETAILS

The CdS samples were nominally undoped single crystals obtained from different commercial suppliers, Eagle Picher and Crystec. The sample from Eagle Picher has a higher purity and a smaller defect content due to differences in the growth method. The samples were oriented with the c axis perpendicular to the external field, averaging the anisotropic contributions of the shallow muonium.

The Si samples were 0.5-mm-thick wafers cut in the 100 plane, obtained commercially from the MTI Corporation. Both crystals were undoped but were grown by different techniques, one by the float zone (FZ) and the other by the Czochralski (CZ) method. The resistivity given by the supplier was >1000 ohm-cm for the FZ sample and 235–250 ohm-cm for the CZ-Si. The CZ-Si is the least pure of the two and contains in particular (electrically inactive) oxygen impurities on the order of 10^{18} cm^{-1}. The Si samples were oriented with the $\langle 100 \rangle$ axis parallel to the external magnetic field. For this orientation, all equivalent 111 bonds corresponding to the main axis of the anisotropic hyperfine interaction have the same angle to the field direction, so that a single value of the hyperfine interaction is expected. Due to a small misalignment a slight splitting occurred and only the summed intensity of the lines was considered in the analysis.

The μSR experiments were performed at the low-temperature facility (LTF) of the Swiss Muon Source, Paul Scherrer Institut, Switzerland. An external magnetic field was applied up to 2 T, perpendicularly to the initial orientation of the muon spin polarization. The time evolution of the muon spin ensemble polarization was measured by detecting the asymmetric emission of decay positrons from muons implanted into the sample.[1,22]

The μSR spectra were fitted in the time domain to a sum of cosine functions of the form $A\cos(2\pi\nu t + \phi)$, where A is the amplitude, ν the frequency, and ϕ the initial phase. For the CdS data a sum of three cosine functions with a Lorentzian envelope was considered, the relaxation of the asymmetry being fixed at the values obtained at 0.01 T. For the Si data, the splitting of the muonium lines yielded up to eight components, in addition to the diamagnetic signal. In order to avoid too many fit parameters, the amplitudes, phases, and relaxation were assumed to be the same for the four lines within the slightly split quartets. This is no limitation in the present context since we are interested only in the sum of the amplitudes in each quartet. In the case of CdS, where the observed frequencies were close to the diamagnetic frequency, a silver calibration in the field range of the experiment was used to correct the amplitudes of the lines for detection efficiency changes at high fields. Because of the larger hyperfine splitting in the case of BC muonium in Si, the silver calibration was not sufficient and a different procedure was necessary, as described below in the data analysis and discussion. The corresponding frequency distributions, used for visualization purposes only, were obtained from the corresponding time spectra using either Fourier analysis or a similar transformation introduced by Lomb.[23]

Radio frequency muon resonance experiments were earlier performed using the HiFi instrument at the ISIS Muon Facility. These used a similar FZ Si wafer, also from the MTI Corporation, cut in the [110] plane, and with a $\langle 110 \rangle$ axis parallel to the external field and initial muon polarization. In this orientation two of the four 111 bonds lie in the plane of the wafer, perpendicular to the field, where their hyperfine splitting is insensitive to small misalignments. The rf coil was formed of thin Cu foil wrapped directly around the 10×10 mm piece of wafer. A fixed frequency of 407 MHz was used, and the field was varied to pick up the lower frequency hyperfine line (at about 3.34 T) and the higher frequency line (2.66 T). Calibration was performed by comparing results taken over the range 2 to 20 K.

III. DATA ANALYSIS AND RESULTS

A. Data analysis

We define the imbalance between the upper and lower hyperfine lines in CdS as $I = (A_3 - A_1)/(A_3 + A_1)$, where A_3 and A_1 are the amplitudes of the higher and lower frequency muonium lines, respectively (Fig. 1). In Si a similar definition is used, but where A_3 and A_1 correspond to the sum of the amplitudes of the split muonium lines higher or lower than the diamagnetic Larmor frequency, respectively (Fig. 2).

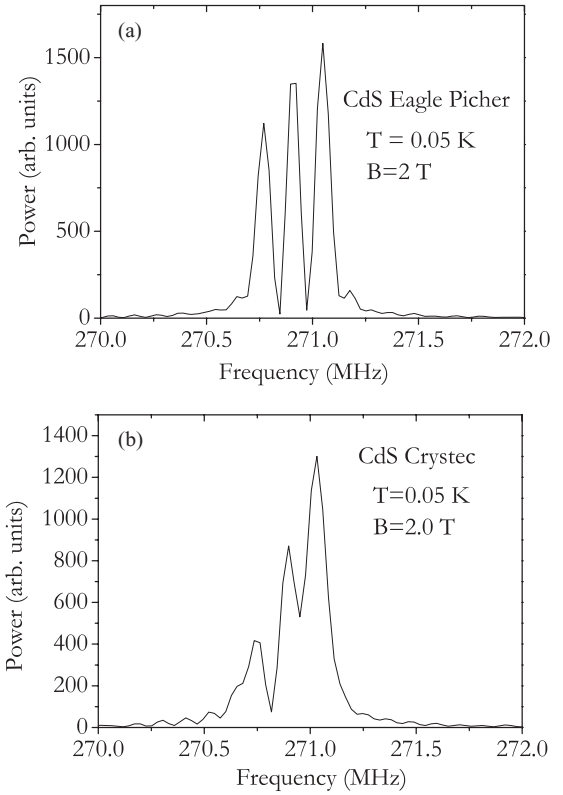

FIG. 1. μSR frequency spectra of CdS measured at low temperature ($T = 0.05$ K) and high magnetic field ($B = 2$ T). (a) CdS (Eagle Picher) sample. (b) CdS (Crystec) sample. The middle line in the spectra corresponds to the diamagnetic muon fraction (Mu^+ or Mu^-) and the two satellite lines correspond to the shallow muonium (Mu^0), the splitting being due to the hyperfine interaction. The intensity difference of the upper and the lower hyperfine line is a direct measure of the electron polarization. Note that the difference is larger (higher polarization) for the Crystec sample than for the Eagle Picher sample.

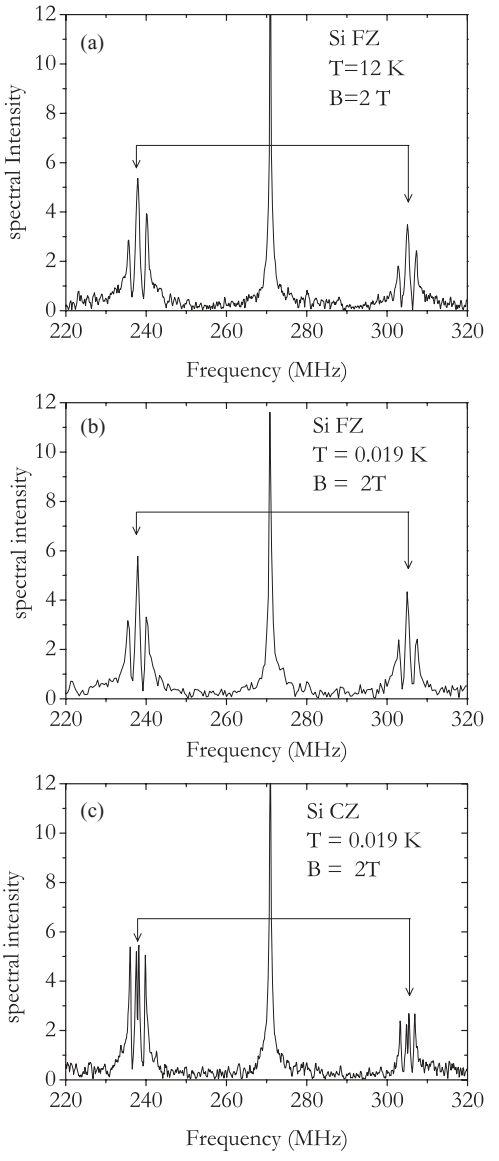

FIG. 2. μSR Fourier spectra of two different Si samples. The upper two spectra (a), (b) are the FZ Si sample measured at two different temperatures (12 K and 0.019 K) and the bottom spectrum (c) is a CZ sample measured at 0.019 K. The external magnetic field was $B = 2$ T. The narrow central line in the spectra corresponds to the diamagnetic fraction (Mu^+ or Mu^-), the quadruplets below and above the central line correspond to BC (anomalous) muonium. Note that the intensity of the upper hyperfine line (sum of the four lines in the quadruplet) is smaller than the intensity of the lower hyperfine line. In panel (a) (used as calibration), the intensity of the upper hyperfine line is reduced due to the finite time resolution of the spectrometer. The two intensities would be equal at 12 K in the absence of this effect. In panel (b), the intensity ratio is about the same as that in the panel (a), thus corresponding to zero polarization. In panel (c), the reduction of the intensity of the upper line is more pronounced than in the calibration spectrum, indicating a nonzero polarization.

The amplitudes were obtained from the fittings in the time domain. If the hyperfine interaction A is positive the higher frequency corresponds to transitions between hyperfine states involving spin-down electrons whereas the lower frequency corresponds to transitions involving spin-up electrons. If the electron g factor is positive it is expected that the population of the electron spin-down state is larger at high fields and low temperatures. The line imbalance is therefore interpreted as an electron spin polarization although its sign may be different from that of the polarization. The sign is the same if the hyperfine interaction is positive but it is inverted if A is negative.

In a transverse field experiment there may also be a small contribution to the imbalance from the dephasing in a delayed conversion between two muonium states which is not related to the electron polarization (see below). The rf experiment in longitudinal field is not affected by this. In the figures we show the measured imbalance rather than the polarization but the discussion is on the physically relevant polarization. In thermodynamical equilibrium, the polarization of a paramagnetic center with $S = 1/2$ is given by the Brillouin function:

$$P = \tanh\left(\frac{g\mu_B B}{2k_B T}\right), \tag{1}$$

where g is the g factor of the state, μ_B the Bohr magneton, k_B the Boltzmann constant, B the external applied magnetic field, and T the temperature. As proposed in previous work[16,21] the data can be described using a modified Brillouin function with two adjustable parameters, α for the saturation value and T_{eff} to adjust the slope, i.e.,

$$P = \alpha \tanh\left(\frac{g\mu_B B}{2k_B T_{\text{eff}}}\right). \quad (2)$$

The hyperfine lines of muonium are well resolved. Thus the observed electron polarization cannot have been built up in the final paramagnetic state because that would cause the smearing out of the hyperfine-split spectral lines. The reduction of the saturation value is therefore attributed to an incomplete polarization buildup in the precursor stage, i.e.,[16]

$$\alpha = \frac{\tau}{\tau + T_1}, \quad (3)$$

where τ is the lifetime of the precursor stage and T_1 is the electron spin-lattice relaxation time in this stage. T_{eff} is the effective temperature, allowed to deviate from the temperature T measured at the sample position. It can be interpreted as a spin temperature, which may differ from the global sample temperature immediately after the implantation.

If the muon lives sufficiently long in a deep muonium precursor state, the muon may experience an appreciable spin precession before converting to the final state. Because of the statistical distribution of the conversion times, this effect leads to a dephasing of the spin precession and consequently to a reduction of the amplitude. The parameters determining the dephasing are $\Delta\omega$ and τ, where $\Delta\omega$ is the difference of the precession angular frequencies in the initial and final state and τ the mean lifetime of the initial state. At low fields, $\Delta\omega$ is different for the two hyperfine lines of the final state and therefore an imbalance (apparent polarization) is observed. The equations describing this effect quantitatively are given in the literature.[24] Evidence of a dephasing effect therefore yields information on the hyperfine constant and lifetime of a precursor state.

B. CdS data

The magnetic field dependence of the imbalance of the shallow muonium lines for both CdS samples is presented in Fig. 3(a). The effect is clearly larger for the CdS (Crystec) sample than for the CdS (Eagle-Picher) sample. In both cases the imbalance is positive and is interpreted as an electron polarization. This polarization is however much lower than expected for a paramagnetic center with $S = 1/2$ in thermodynamical equilibrium. The data was therefore fitted with the modified Brillouin function [Eq. (2)]. The known value of the g factor for conduction band electrons in CdS is close to 2 (Refs. 25 and 26) and $g = 2$ was used in the modified Brillouin function. The results of the fitted parameters α and T_{eff} are presented in Table I. Saturation values below unity indicate an incomplete buildup of the electron spin polarization, which is more pronounced in the CdS (Eagle Picher) sample. The effective temperature is similar for both samples within the fitting uncertainty and it is more than 20 times larger than the temperature measured at the sample position. The samples have a low thermal conductivity and a temperature difference between the sample and the temperature sensor is likely to occur. However, the difference is so large that it is plausible that this effective temperature corresponds to a local temperature of the electron spin system. The electrons available for muon capture are mainly the radiolytic electrons ejected from the valence band, unpolarized, due to muon implantation.

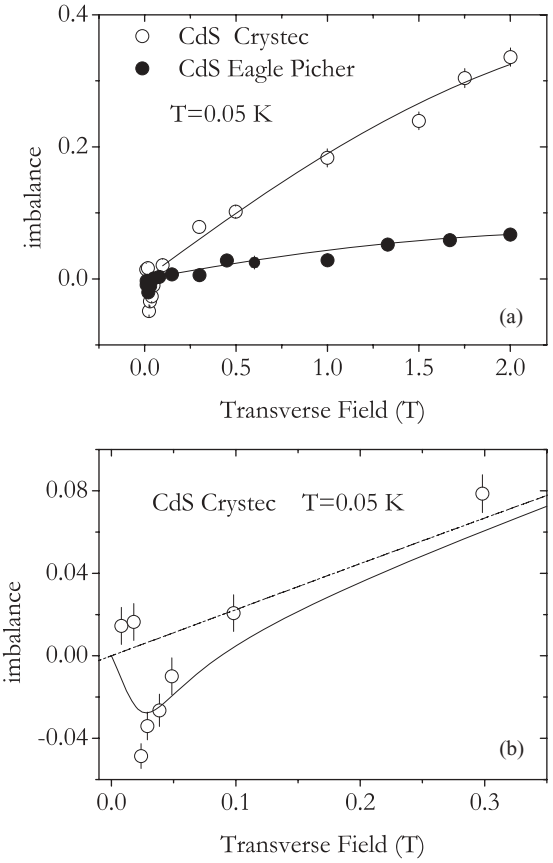

FIG. 3. (a) Imbalance (corresponding to the electron spin polarization) for the two nominally undoped CdS samples from different suppliers, Crystec (open circles) and Eagle Picher (solid circles), as a function of the applied magnetic field. The temperature of the samples was $T = 0.05$ K. The solid lines are fits with the modified Brillouin function [Eq. (2)]. (b) Detail of panel (a) at low fields showing the negative values of imbalance in CdS (Crystec) at low fields. The undershoot is attributed to a dephasing caused by the preceding μSR in the precursor state. The solid line shows a fit within this model (see Sec. III A). The modified Brillouin-like behavior (dashed line) was taken into account in the fit. The fit parameters (hyperfine interaction and mean lifetime) for the deep muonium precursor are $A = 980 \pm 600$ MHz and $\tau = 0.3 \pm 0.2$ ns.

TABLE I. Fit parameters T_{eff} and α obtained from the analysis of the CdS data using a modified Brillouin function [Eq. (2)]. The electron g factor was set to 2. The temperature measured with the temperature sensor at the sample position was $T = 0.05$ K.

Sample	T_{eff} (K)	α
CdS Crystec	1.5(5)	0.4(2)
CdS Eagle Picher	1.1(5)	0.08(5)

The observed imbalance of shallow muonium lines is positive for most of the field range but at low fields (below 0.1 T) there is an inversion of sign [Fig. 3(b)]. This effect is quite small and has been observed before for the CdS (Eagle Picher) sample only, yielding a hyperfine interaction $A = 500 \pm 300$ MHz and an average lifetime $\tau = 0.3 \pm 0.2$ ns for the precursor state.[16] We have now confirmed this effect measuring the CdS (Crystec) sample. This sign inversion effect is attributed to dephasing due to the conversion between a short-lived precursor state and the final shallow state. The analysis of the new CdS (Crystec) data using the same models from the literature[24] used previously[16] yields a hyperfine interaction $A = 980 \pm 600$ MHz and an average lifetime $\tau = 0.3 \pm 0.2$ ns for the precursor state. These values are basically consistent with the previous result.

The formation probability of the different muonium states is also sample dependent (Fig. 4), and the CdS (Eagle Pitcher) sample shows a smaller polarization but a larger paramagnetic fraction. Above 1 T there is a slight increase of the paramagnetic fraction with increasing magnetic field, which is more pronounced for the Crystec sample.

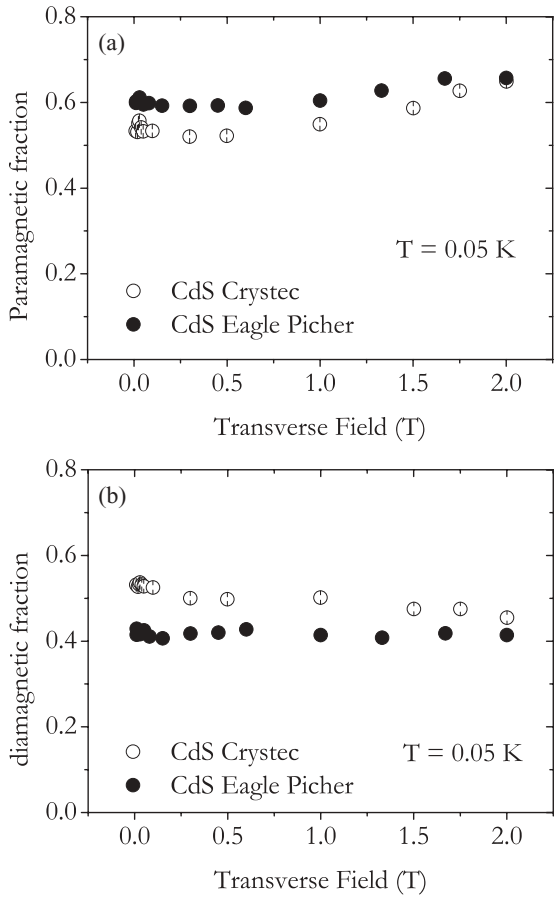

FIG. 4. Formation probability (fraction) of the different muon states in two different CdS samples from different suppliers, Eagle Picher (closed circles) and Crystec (solid circles) at $T = 0.05$ K. The paramagnetic fraction (a) corresponds to shallow muonium and the diamagnetic fraction (b) to Mu^+ or Mu^-.

C. Si TF data

Figure 2 shows the frequency distributions for the two Si samples in an external transverse magnetic field of 2 T. The measured temperatures were 12 K and 0.019 K for the Si (FZ) sample ($\rho > 1000$ ohm-cm) and 0.019 K for the Si (CZ) sample ($\rho \approx 235$–250 ohm-cm). They correspond to a high-field pattern with a set of BC muonium lines on either side of the central diamagnetic line. The total summed amplitude for each set of muonium lines was considered for the calculation of the imbalance between the lower and the upper hyperfine lines. At 12 K negligible polarization is expected and the observed imbalance in the Fig. 2(a) is therefore purely instrumental, arising from detection efficiency changes at high fields and finite time resolution. Comparing the Figs. 2(b) and 2(c) with the calibration at 12 K [Fig. 2(a)] we conclude that only the Si CZ sample shows a nonzero polarization. The amplitudes of the upper and lower hyperfine lines at 0.019 K were corrected using the 12 K data as a calibration. The results for the corrected imbalance at 0.019 K are plotted in Fig. 5. The hyperfine constant of BC muonium in Si is known to be negative for all orientations[1,27] so that the polarization has the opposite sign of the imbalance. No polarization is observed for the Si FZ sample within the experimental errors, whereas a clear effect is present in the Si CZ sample, the less pure sample. The current Si CZ data do not allow us to determine the saturation value and it is not possible to fit a modified Brillouin function. However, the fact that the saturation is not achieved at 1 T indicates that the effective temperature T_{eff} must be much larger than the measured temperature, of the order of 1 K or above. A modified Brillouin function corresponding to a temperature of 2 K is plotted in Fig. 5 as a guide to the eye.

The formation probability of the muonium states in Si is also sample dependent (Fig. 6) and the sample with larger polarization presents a smaller paramagnetic fraction, similar to the trend observed in CdS. The diamagnetic fractions at 1 and 2 T are identical for both the Si CZ and Si FZ samples, within the errors. At 0.1 T only the Si CZ sample was measured.

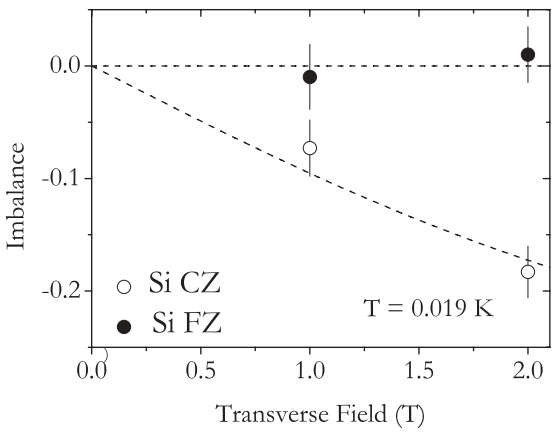

FIG. 5. Imbalance (symmetric to the electron spin polarization, as explained in the text) of BC muonium for two different Si samples at $T = 0.019$ K as a function of the applied magnetic field. For the Si CZ sample a clear polarization is observed, whereas for the Si FZ sample the polarization is zero within the experimental errors. The dashed line for the Si CZ sample corresponds to a modified Brillouin function with $T_{\text{eff}} = 2$ K and $\alpha = -0.3$ and is a guide to the eye only.

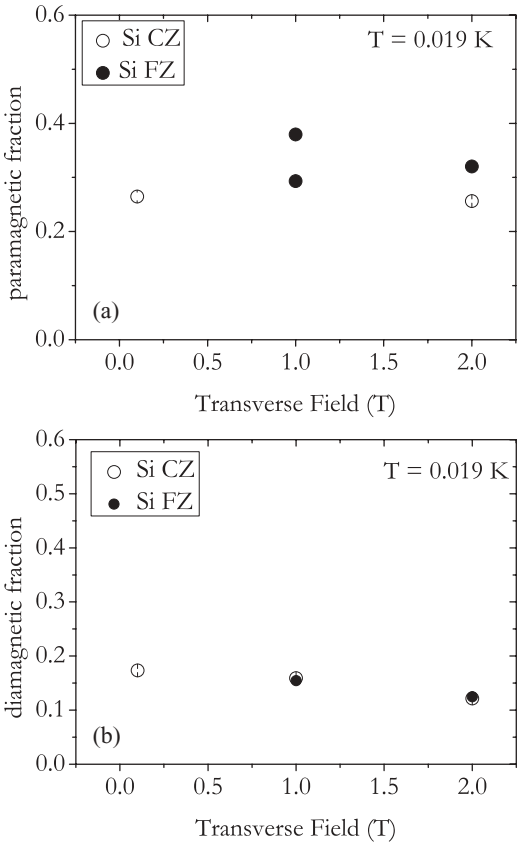

FIG. 6. Formation probability (fraction) of the different muon states for two different Si samples, CZ (open circles) and FZ (solid circles). The paramagnetic fraction (a) corresponds to BC (anomalous) muonium and the diamagnetic fraction (b) to Mu^+ or Mu^-.

D. Si rf data

The rf coil was set up for a fixed frequency (407 MHz) and power level. For each of the two resonance lines we scanned the magnetic field through the line, measuring with rf on and off to correct for any background drifts. Measurements were taken at

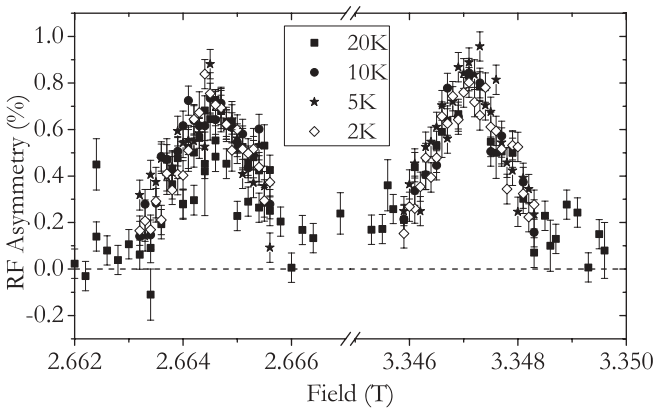

FIG. 7. Resonance lines for BC muonium in the (111) sites perpendicular to the field applied along (110). The lower (upper) line here corresponds to the upper (lower) frequency sideband in the TF spectrum. The central diamagnetic line at about 3.00 T, and lines from other (111) orientations at 35° to B_0 (2.85 and 3.15 T) were not measured.

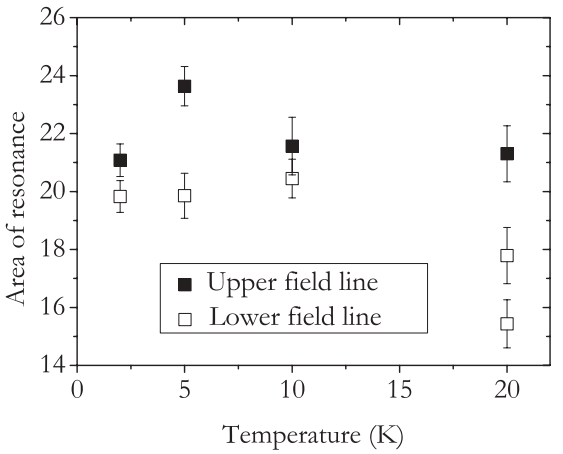

FIG. 8. Fitted areas of the lines as a function of temperature, keeping the linewidth fixed. No polarization (within errors) was detected in this sample, agreeing with the transverse field result of the FZ Si sample.

a series of temperatures from 2 K to 20 K (Fig. 7). Inspection of the time domain data on-resonance shows a precession in the rf field B_1 of about 5×10^{-4} T; however, this is strongly damped due to inhomogeneity. The resonance curves were generated using time-integral asymmetry.

Instrumental effects may cause the fraction of muons landing on the sample to differ between the two resonance fields, and the detector efficiency may also vary. Therefore we used the 20 K data as a "zero polarization" reference. No polarization (within errors) was detected in this sample, thus backing up the null result obtained in the transverse field experiment on this material (Fig. 8) and showing that in this case no additional polarization is introduced as a result of delayed conversion.

IV. DISCUSSION

We assume, as in our earlier publication,[16] that the electron spin polarization of muonium in these samples takes place in an intermediate stage which exists for several hundreds of picoseconds between implantation of the positively charged muon and the formation of the final neutral state. The basis for this assumption is not only the fact that the samples are nonmagnetic, so that no polarized electrons can be captured in the course of the implantation of muons, but also the observation that the hyperfine lines of the final muonium state are well resolved, showing no evidence of the existence of a fast spin-flip rate, as expected if the polarization buildup happened after the formation of the final state. The polarization must therefore be established during the lifetime of the precursor stage before the formation of the final state.

Two different routes for the formation of shallow muonium were identified:[16] (i) formation by capture of an electron from the conduction band and (ii) formation via conversion from a precursor state. In the former case the polarization of the electron spin is built up in the conduction band, prior to the capture by the muon; in the latter route, the polarization is built up in a neutral precursor muonium state. At the low temperatures of these experiments, the electrons present at the

conduction band arise mainly from the ionization processes occurring during the muon implantation process.

In CdTe[16] the two processes could be distinguished since the sign of the g factor and consequently the sign of polarization were different for the two processes. This is not the case in the current experiments: the electron g factor is expected to be positive and close to 2 for both routes either in CdS[2,25,26] or in Si.[2,28] Our data confirm the presence of a deep, short-lived precursor muonium state in CdS [Fig. 3(b)], as had been found in a different CdS sample.[16] However, no significant missing fraction is observed in CdS which indicates that the fraction of shallow muonium formed via a deep, short-lived precursor must be small (less that 20%). Electric field experiments[15] also indicate that electron capture from the conduction band is the dominant route in CdS. Furthermore, these experiments suggest paramagnetic muonium in CdS is formed in a very weakly bound state, which may not be in its final configuration. Electric field experiments in Si (Ref. 19) suggest, on the other end, that neutral BC muonium (Mu^0_{BC}) is formed by electron capture when the positive muon is already in its final configuration at the bond-center site, Mu^+_{BC}.

The electron polarization is particularly sensitive to the processes occurring in the course of the precursor stage, but the formation probabilities of the different final states also provide important information about this stage. For the interpretation of the data, we suggest the following picture for the precursor stage: The implanted muon comes to rest at an interstitial site in the unrelaxed lattice. The lattice reacts to the presence of the impurity and starts to relax, driven by the energy gain in the configuration change, and the muon migrates to the final bound position. The total energy of the system is a function of the reaction coordinate and may show a flat region or a small barrier retarding the transformation to the final configuration. The binding energy of the electron to the positive muon is of special interest here. If this energy level comes close to the conduction band during the transformation, a thermally activated redistribution of the electron between the bound state and the conduction band may take place (electron loss or electron capture). The system tries to establish a Boltzmann distribution but the available time is probably too short in order to fully reach equilibrium. In the subsequent fast change to the final configuration, the distribution between muonium and bare muon is frozen in, resulting in the final fractions of paramagnetic and diamagnetic states. Some details of the process, namely whether the electron capture occurs in the final site/configuration or in an intermediate configuration, may differ from one system to another and even within a system different routes may coexist.

The present experiment shows again that the electron polarization of muonium is rather low, certainly much lower than expected for a paramagnetic impurity in thermal equilibrium at low temperatures and high magnetic fields. This is not surprising considering the small time window available for the buildup process.

Additionally, three different effects became apparent from the current experiments.

(1) The polarization depends on the impurity/defect content of the sample: it is larger if the sample is less pure [Figs. 3(a) and 5]. An interaction with defects in the sample may shorten the electron spin-lattice relaxation time T_1.[16] Moreover, if the formation route is via electron capture from the conduction band, a longer delay time τ for electron capture may occur if, due to defects, electron-hole recombination decreases the number of electrons available for capture and therefore extends the time available for electron polarization. If the formation route is via a precursor state, an increase of its lifetime τ may still occur if the presence of defects increases the energy barrier in the transformation path for the final configuration. Both an increase of τ and a decrease of T_1 would contribute to a larger α in Eq. (3).

(2) The formation probability of bound (paramagnetic) muonium is also sample dependent and it is smaller for the less pure sample [Figs. 4(a) and 6(a)]; i.e., the presence of defects enhances polarization but reduces the yield of bound muonium. It is possible that the electron mobility in the conduction band is reduced for the less pure samples, lowering the probability of electron capture in addition to increasing the time for electron polarization in the conduction band. Another possibility is that the probability of formation of bound muonium is influenced by changes in the transition path to its final configuration, caused by defects. Examples of possible changes that would reduce the formation probability of bound muonium are an increase in the energy barrier along the path or a shift of the single electron level closer to the conduction band.

(3) Experimentally, a magnetic field dependence of the formation probability of the different muon states is evident in CdS: the paramagnetic (bound) muonium fraction observed in the transverse field increases and the diamagnetic fraction tends to stay constant or to decrease with increasing field. In Si the information is scarce and the absolute fractions are not very precise due to corrections of the amplitudes with the Ag calibration. A magnetic-field-dependent decrease of the diamagnetic fraction was also observed in GaAs.[18] A possible explanation is to assume that the electrons in the conduction band are in Landau levels and that at least the zero point level has to be excited in the ionization process. This energy is

$$\frac{1}{2}\hbar\omega_c = \frac{1}{2}\hbar\frac{eB}{m}, \tag{4}$$

where ω_c is the cyclotron frequency and m the effective electron mass. For $m = 0.2m_0$ and $B = 1$ T, this yields an energy of the order of 0.29 meV. Thus, an energy which depends on the magnetic field is needed to promote an electron from a bound state into the conduction band. This effect becomes appreciable if the muonium electron level is close to the conduction band (which may happen during the site transformation) and stabilizes paramagnetic muonium, favoring muonium formation at the expense of the diamagnetic (bare muon) fraction. Such a tendency is observed experimentally in CdS.

V. CONCLUSIONS

The observation of an electron polarization in bound (anomalous) muonium in Si is particularly interesting since most other properties of this state have been studied extensively in the past[1,2] but no polarization had been reported before. Thus the present results on the polarization constitute new information on the muonium states in Si. This information is

important because it shows the possibility of understanding the formation of muonium states in silicon.

We find that the polarization in Si is very small: it is zero within errors for the very pure Si-FZ sample but it is clearly present for the less pure Si-CZ sample. In fact, the results in CdS and Si show similar general trends for the electron polarization of bound muonium: the electron polarization is lower than the equilibrium value and it is larger for samples with higher contents of impurities/defects. In addition, in both systems the formation probability of the bound muonium state is found to be smaller in samples with higher contents of impurities/defects.

The results fit into a general picture whereby the electron polarization of the observed final state is built up in a precursor stage(with a lifetime $\tau \approx 300$ ps) influenced by pre-existing defects or impurities. Mobile atomic muonium can partially acquire this polarization prior to self-trapping in the lattice, as can radiolytic electrons prior to Coulomb capture by the positive ion. This precursor stage plays a decisive role for the properties observed experimentally. Considering the significant differences between the final muonium configurations in Si and CdS the general picture here described may be of far wider use in the modeling of muonium formation in semiconductors. The development of such a model is essential for the interpretation of the final muonium configurations and their analogy with isolated hydrogen centers.

ACKNOWLEDGMENTS

We are grateful to the PSI machine and beamline groups whose outstanding efforts have made these experiments possible. We would like to thank Chris Baines for his support in setting up the beamline and cryostat. This research project has been supported by the European Commission under the 6th Framework Programme through the Key Action: Strengthening the European Research Area, Research Infrastructures, Contract No. RII3-CT-2004-505925. CEMDRX was supported by FCT (Portugal) under COMPETE: PEst-/FIS/UI0036/2011 Strategic Project.

*lena@fis.uc.pt

†[Also at]E.S.Te.S.C., Polytechnic Institute of Coimbra, P-3040-854 Coimbra, Portugal.

[1] S. F. J. Cox, Rep. Prog. Phys. **72**, 116501 (2009).

[2] B. D. Patterson, Rev. Mod. Phys. **60**, 69 (1988).

[3] R. L. Lichti, K. H. Chow, and S. F. J. Cox, Phys. Rev. Lett. **101**, 136403 (2008).

[4] B. E. Schultz, K. H. Chow, B. Hitti, R. F. Kiefl, R. L. Lichti, and S. F. J. Cox, Phys. Rev. Lett. **95**, 086404 (2005).

[5] S. F. J. Cox, E. A. Davis, S. P. Cottrell, P. J. C. King, J. S. Lord, J. M. Gil, H. V. Alberto, R. C. Vilão, J. Piroto Duarte, N. Ayres de Campos, A. Weidinger, R. L. Lichti, and S. J. C. Irvine, Phys. Rev. Lett. **86**, 2601 (2001).

[6] J. M. Gil, H. V. Alberto, R. C. Vilão, J. P. Duarte, P. J. Mendes, L. P. Ferreira, N. Ayres de Campos, A. Weidinger, J. Krauser, C. Niedermayer, and S. F. J. Cox, Phys. Rev. Lett. **83**, 5294 (1999).

[7] J. M. Gil, H. V. Alberto, R. C. Vilão, J. Piroto Duarte, N. Ayres de Campos, A. Weidinger, J. Krauser, E. A. Davis, S. P. Cottrell, and S. F. J. Cox, Phys. Rev. B **64**, 075205 (2001).

[8] R. C. Vilão, J. M. Gil, A. Weidinger, H. V. Alberto, J. Piroto Duarte, N. Ayres de Campos, R. L. Lichti, K. H. Chow, S. P. Cottrell, and S. F. J. Cox, Phys. Rev. B **77**, 235212 (2008).

[9] R. C. Vilão, H. V. Alberto, J. P. Duarte, J. M. Gil, A. Weidinger, N. Ayres de Campos, R. L. Lichti, K. H. Chow, and S. F. J. Cox, Phys. Rev. B **72**, 235203 (2005).

[10] E. L. Silva, A. G. Marinopoulos, R. C. Vilão, R. B. L. Vieira, H. V. Alberto, J. Piroto Duarte, and J. M. Gil, Phys. Rev. B **85**, 165211 (2012).

[11] R. C. Vilão, A. G. Marinopoulos, R. B. L. Vieira, A. Weidinger, H. V. Alberto, J. P. Duarte, J. M. Gil, J. S. Lord, and S. F. J. Cox, Phys. Rev. B **84**, 045201 (2011).

[12] P. D. C. King, R. L. Lichti, Y. G. Celebi, J. M. Gil, R. C. Vilão, H. V. Alberto, J. Piroto Duarte, D. J. Payne, R. G. Egdell, I. McKenzie, C. F. McConville, S. F. J. Cox, and T. D. Veal, Phys. Rev. B **80**, 081201 (2009).

[13] S. F. J. Cox, J. S. Lord, S. P. Cottrell, J. M. Gil, H. V. Alberto, A. Keren, D. Prabhakaran, R. Scheuermann, and A. Stoykov, J. Phys.: Condens. Matter **18**, 1061 (2006).

[14] S. F. J. Cox, J. L. Gavartin, J. S. Lord, S. P. Cottrell, J. M. Gil, H. V. Alberto, J. P. Duarte, R. C. Vilo, N. A. de Campos, D. J. Keeble, E. A. Davis, M. Charlton, and D. P. van der Werf, J. Phys.: Condens. Matter **18**, 1079 (2006).

[15] D. G. Eshchenko, V. G. Storchak, S. P. Cottrell, and S. F. J. Cox, Phys. Rev. B **68**, 073201 (2003).

[16] H. V. Alberto, A. Weidinger, R. C. Vilão, J. P. Duarte, J. M. Gil, J. S. Lord, and S. F. J. Cox, Phys. Rev. B **81**, 245205 (2010).

[17] R. Kadono, A. Matsushita, R. M. Macrae, K. Nishiyama, and K. Nagamine, Phys. Rev. Lett. **73**, 2724 (1994).

[18] V. G. Storchak, D. G. Eshchenko, and J. H. Brewer, J. Phys.: Condens. Matter **16**, S4761 (2004).

[19] V. Storchak, S. F. J. Cox, S. P. Cottrell, J. H. Brewer, G. D. Morris, D. J. Arseneau, and B. Hitti, Phys. Rev. Lett. **78**, 2835 (1997).

[20] T. Prokscha, E. Morenzoni, D. G. Eshchenko, N. Garifianov, H. Glückler, R. Khasanov, H. Luetkens, and A. Suter, Phys. Rev. Lett. **98**, 227401 (2007).

[21] H. V. Alberto, A. Weidinger, R. C. Vilão, J. P. Duarte, J. M. Gil, N. A. de Campos, J. S. Lord, and S. F. J. Cox, Phys. B: Condens. Matter **404**, 5110 (2009).

[22] K. H. Chow, B. Hitti, and R. F. Kiefl, in *Identification of Defects in Semiconductors*, edited by M. Stavola, Semiconductors and Semimetals Vol. 51A (Academic Press, San Diego, 1998).

[23] N. Lomb, Astrophys. Space Sci. **39**, 447 (1976).

[24] E. Roduner, *The Positive Muon as a Probe in Free Radical Chemistry*, Lecture Notes in Chemistry (Springer Verlag, Berlin, 1988).

[25] J. S. Lord, S. F. J. Cox, H. V. Alberto, J. P. Duarte, and R. C. Vilão, J. Phys.: Condens. Matter **16**, S4707 (2004).

[26] M. Willatzen, M. Cardona, and N. E. Christensen, Phys. Rev. B **51**, 17992 (1995).

[27] K. H. Chow, R. F. Kiefl, B. Hitti, T. L. Estle, and R. L. Lichti, Phys. Rev. Lett. **84**, 2251 (2000).

[28] D. K. Wilson and G. Feher, Phys. Rev. **124**, 1068 (1961).